Published in final edited form as:
J Comp Neurol. 2011 September 1; 519(13): 2658–2676. doi:10.1002/cne.22654.

Distribution and physiological effects of B-type allatostatins (myoinhibitory peptides, MIPs) in the stomatogastric nervous system of the crab, *Cancer borealis*

Theresa M. Szabo[1,4], **Ruibing Chen**[2,3], **Marie L. Goeritz**[1], **Ryan T. Maloney**[1], **Lamont S. Tang**[1,5], **Lingjun Li**[2], and **Eve Marder**[1]

[1]Volen Center and Department of Biology, Brandeis University, Waltham, MA, USA

[2]School of Pharmacy and Department of Chemistry, University of Wisconsin-Madison, Madison, WI, USA

[3]Research Center of Basic Medical Sciences, Tianjin Medical University, Tianjin, P. R. China 300070

Abstract

The crustacean stomatogastric ganglion (STG) is modulated by a large number of amines and neuropeptides that are found in descending pathways from anterior ganglia or reach the STG via the hemolymph. Among these are the allatostatin (AST) – B types also known as myoinhibitory peptides (MIPs). We used mass spectrometry to determine the sequences of nine members of the AST-B family of peptides that were found in the stomatogastric nervous system of the crab, *Cancer borealis*. We raised an antibody against *Cancer borealis* Allatostatin-B1 (CbAST-B1) (VPNDWAHFRGSWa) and used it to map the distribution of CbAST-B1-like immunoreactivity (-LI) in the stomatogastric nervous system. CbAST-B1-LI was found in neurons and neuropil in the commissural ganglia (CoGs), in somata in the esophageal ganglion (OG), in fibers in the stomatogastric nerve (*stn*), and in neuropilar processes in the STG. CbAST-B1-LI was blocked by preincubation with 10^{-6} M CbAST-B1, and partially blocked by lower concentrations. Electrophysiological recordings of the effects of CbAST-B1, CbAST-B2, and CbAST-B3 on the pyloric rhythm of the STG showed that all three peptides inhibited the pyloric rhythm in a state-dependent manner. Specifically, all three peptides at 10^{-8} M significantly decreased the frequency of the pyloric rhythm when the initial frequency of the pyloric rhythm was below 0.6 Hz. These data suggest important neuromodulatory roles for the CbAST-B family in the stomatogastric nervous system.

Keywords

neuropeptides; peptide sequencing; immunocytochemistry; pyloric rhythm; matrix-assisted laser desorption/ionization time-of-flight (TOF)/TOF mass spectrometry (MALDI TOF/TOF MS)

Address all correspondence to Eve Marder, Volen Center, MS 013, Brandeis University, 415 South St, Waltham, MA 02454, Phone: (781) 736-3140, FAX: (781) 736-3142, marder@brandeis.edu.
[4]Present address: Department of Biological Sciences, Delaware State University, 1200 N DuPont Highway, Dover, DE 19901-2277
[5]Present address: Department of Biochemistry & Biophysics, Box 2822, 1550 4th St, Rock Hall-MB RH448, UCSF, San Francisco, CA 94143

Introduction

The crustacean stomatogastric nervous system (STNS) contains a large number of amines and neuropeptides (Harris-Warrick and Marder, 1991; Harris-Warrick et al., 1992; Marder and Bucher, 2007; Marder and Thirumalai, 2002; Marder and Weimann, 1992; Nusbaum, 2002; Nusbaum and Beenhakker, 2002; Stein, 2009). Advances in mass spectrometry and genome sequencing have catalyzed an explosion of data characterizing the neuropeptidome in many animals, including crustaceans (Boonen et al., 2008; Chen et al., 2010; Christie et al., 2008; Clynen et al., 2010; Dickinson et al., 2009a; Fu et al., 2005a; Fu et al., 2005b; Ma et al., 2009a; Ma et al., 2008; Ma et al., 2010; Williamson et al., 2001). As a consequence of the biochemical and electrophysiological experiments, we now know that neuronal circuits and neuromuscular junctions are modulated by a large number of different substances (Cruz-Bermudez and Marder, 2007; Jorge-Rivera et al., 1998; Marder and Bucher, 2007; Nusbaum and Beenhakker, 2002; Nusbaum et al., 2001).

The allatostatins (ASTs) are neuropeptides that have important neuromodulatory roles in arthropods. Peptides were initially termed “allatostatins” by virtue of their inhibition of juvenile hormone (JH) production in the corpora allata of insects; however, JH is not found in crustaceans. ASTs regulate a range of important processes and can act as inhibitors of endocrine function, as neuromodulators, on muscle, and directly on metabolic pathways (Audsley et al., 2008; Audsley and Weaver, 2003; 2009; Bendena et al., 1999; Stay and Tobe, 2007; Weaver and Audsley, 2009). Three families of different pepties have been called ASTs, althought they have no sequence homology and are unrelated: 1) A-types, first isolated from cockroach, that possess the sequence Y/FXFGL-NH_2 (Pratt et al., 1989; Woodhead et al., 1989), 2) B-types, first isolated from cricket, with the sequence $W(X)_6$Wamide (Williamson et al., 2001), and 3) C-types, first isolated from the Lepidopterans, with a PISCF sequence (Jansons et al., 1996; Kramer et al., 1991). These peptides possess similar physiological functions but lack any sequence similarity, suggesting that there has been convergent evolution of their function at least three times, highlighting the importance of allatostatic substances in arthropods.

Although ASTs were first identified in insects, all three classes of peptides have since been identified in crustaceans (Dickinson et al., 2009b; Duve et al., 1997; Duve et al., 2002; Fu et al., 2005b; Huybrechts et al., 2003; Stemmler et al., 2010), where their physiological roles are just beginning to be understood (Dircksen et al., 1999; Fu et al., 2007; Jorge-Rivera, 1997; Kreissl et al., 1999; Ma et al., 2009b). One known function is stimulating the production of methyl farnesoate (MF) from farnesoic acid by the mandibular organs, the crustacean homolog of the insect corpora allata (Kwok et al., 2005). MF modulates molting and reproduction in crustaceans in a manner similar to JH regulation of these processes in insects (Bendena et al., 1999; Stay and Tobe, 2007; Tobe and Bendena, 1999). In addition, B-type ASTs are known for their myoinhibitory role and are therefore also referred to as myoinhibitory peptides (MIPs) (Nassel and Winther, 2010). For consistency with other recent studies in crustaceans (Christie et al., 2010), here we will refer to the peptides as allatostatins.

Members of all three AST families are present in the crab, *C. borealis*, and have been shown to regulate neuronal function in the STNS (Fu et al., 2007; Ma et al., 2009b; Skiebe and Schneider, 1994). Specifically, the three ASTs reduce pyloric network burst frequency in a state-dependent manner; the faster the initial burst frequency, the less effective the AST peptide. Because peptides from the three AST families lack sequence similarity, their inhibition of the pyloric rhythm is likely not due to their action on the same receptor families; instead, it is more likely that they share some downstream targets. Thus, an

examination of the distribution of these peptides and their potential targets might provide an explanation for the apparent similarities in their actions.

Methods

Animals and dissections

Adult *Cancer borealis* were obtained from Commercial Lobster (Boston, MA, USA). All animals were maintained in artificial sea water tanks at approximately 11°C without food on a 12 hr light / 12 hr dark cycle. Dissections of the STNS were performed as previously described (Goaillard et al., 2004) in chilled physiological saline (*C. borealis* (mM): NaCl, 440; KCl, 11; $MgCl_2$, 26; $CaCl_2$, 13; Trizma base, 11; maleic acid, 5; pH 7.45).

Antibody characterization

Peptide CbAST-B1 (VPNDWAHFRGSW) was synthesized by the Biotechnology Center at the University of Wisconsin-Madison. The peptide was conjugated to bovine serum albumin (BSA) using the carbodiimide procedure (1-Ethyl-3-(3-dimethylaminopropyl)carbodiimide hydrochloride) (Lampire Biological Laboratories). Following a preimmune bleed, BSA-linked peptide (0.5 mg in 500 μL Freund's complete adjuvant) was injected subcutaneously into New Zealand white rabbits (Lampire Biological Laboratories, Hypersville, PA). Rabbits were boosted with BSA-linked peptide (0.5 mg in 500 μl Freund's incomplete adjuvant) 3 and 6 weeks later before the first production bleed at day 50. Antibody production was verified and measured using ELISAs. This antibody will be referred to as a CbAST-B1 antibody throughout the remainder of the study (Table 1). The ELISA design involved capture of the specific antibody by a target antigen coated on 96 well microtiter plates. Wells were coated with target antigen at 1 μg/well (antigen was diluted in 50 mM Carbonate at pH 7.6). Antisera were diluted in ten-fold serial dilutions using 1% BSA in phosphate buffered saline (PBS). Specific antibody was detected by goat anti-rabbit IgG secondary antibody conjugated to horseradish peroxidase (HRP). The signal was developed using (2,2′-Azinobis [3-ethylbenzothiazoline-6-sulfonic acid]-diammonium salt) (ABTS) substrate. The reaction was stopped after 20 minutes and absorbance at 405nm was measured.

A-type AST monoclonal antibodies were made against *Diploptera punctata* (Dippu) AST- 7 (APSGAQRLYGFGL-NH2; N-terminal coupled to BSA) and obtained from the Developmental Studies Hybridoma Bank, University of Iowa (Stay et al., 1992) (Table 1). Specificity of this antibody for AST-7 (previously called AST I) was demonstrated using ELISA competition assays in which the antibody was preincubated with 5 different synthetic AST peptides, including APSGAQRLYGFGL-NH2 (Stay et al., 1992) and the presence and distribution of immunoreactivity throughout the STNS of *C. borealis* to AST-7 (APSGAQRLYGFGL-NH2) using a rabbit polyclonal has previously been demonstrated (Skiebe and Schneider, 1994).

CabTRP-like immunoreactivity was examined with a rat monoclonal anti-substance P antibody (clone NC1/34HL), obtained from Accurate Chemical and Scientific, Westbury, NY (Table 1). The antibody was made against Substance P, conjugated to BSA with carbodiimide as coupling agent and recognizes the COOH-terminal part of substance P (Cuello et al., 1979). The specificity of clone NC1/34HL for CabTRP1a in *C. borealis* (Table 1) was previously shown by preabsorption controls with CrabTRP1a peptide (sequence APSGFLGMR-NH2) (Christie et al., 1997). In this previous study, also done in *C. borealis* the authors showed that 10^{-4} M CabTRP1a completely blocked all of the staining revealed by 1:300 dilution of clone NC1/34HL (the same antibody and dilution used in this study). The distribution of immunoreactivity with clone NC1/34HL in the STNS of *C.*

borealis has been characterized (Blitz et al., 1995; Christie et al., 1997; Goldberg et al., 1988). The same distribution was seen in this study.

Immunocytochemistry

C. borealis were examined to determine the distribution of the A- and B-type AST-LI as well as CabTRP-like immunoreactivity in the STNS (n=36). Dissected nervous systems were fixed for 30-60 minutes using 4% paraformaldehyde in 0.1M phosphate buffered saline (PBS; 440 mM NaCl, 11 mM KCl, 10 mM Na_2HPO_4, 2 mM KH_2PO_4; pH 7.4-7.5). After fixation, preparations were washed 4× in PBS, then stored for 0-7 days at 4°C before processing. Prior to application of the antibody, preparations were washed 4× for 15 minutes in PBS-T (0.3-1% Triton-X 100 in PBS). PBS-T containing 5% Normal Goat Serum (NGS) and 1-5% BSA was then applied for two hours, followed by 4 additional 15 minute washes in PBS-T alone. Antibodies against A- and B-type ASTs were applied overnight at a concentration of 1:500 – 1:1000 in PBS-T with 5% NGS and 1% BSA at room temperature, following which preparations were washed 4-8× for 15 min. CabTRP-like immunoreactivity was studied with 1:300 dilution of anti-substance P monoclonal antibody (clone NC1/34HL, Table 1) with 5% NGS and 1% BSA overnight at room temperature. For blocking studies, CbAST-B1 antibody was preincubated for 1 hour at 1:1000 with 10^{-4} to 10^{-9} M CbAST-B1 peptide to determine the effectiveness of the antibody. Additionally, 10^{-4} M CbAST-B2 peptide, 10^{-4} M CbAST-B3 peptide, or 10^{-4} M Dippu-AST-3 peptide (Bachem, Torrance, CA) were preincubated with the CbAST-B1 antibody for 1 hour to determine the specificity of binding. All CbAST-B-type peptides were synthesized by the Biotechnology Center at the University of Wisconsin-Madison.

Polyclonal antibodies against mouse or rabbit (raised in either goat or donkey; Invitrogen) were used to visualize A- and B-type antibodies. These antibodies were conjugated to Alexa Fluor dyes with optimal excitation wavelengths ranging from 488-647 nm. They were applied to the preparations at a concentration of 1:500 in PBS-T for two to three hours at room temperature. Preparations were then washed 4 times for 15 minutes in PBS-T, followed by four washes of 15 minutes in PBS. They were then mounted in ProLong Gold Antifade Reagant (Invitrogen) or Vectashield (Vector Laboratories).

Soma fills

Somata were filled with 4% neurobiotin tracer (Vector Laboratories) in 50mM Tris buffer and 0.5M KCl, or with 10 mM Alexa Fluor 568-hydrazide potassium salt. Low resistance recording electrodes were backfilled for 10 minutes with the tracer. For neurobiotin fills, the shaft of the electrode was filled with 2 M KCl, leaving a gap of ~ 1 cm between the neurobiotin solution in the tip. Neurobiotin was injected for 30 minutes using positive current pulses of 3 to 6 nA, 500 ms duration, 0.3 Hz. Alexa Fluor hydrazide was injected for 30 minutes with negative pulses of -3 to -11 nA, 500ms duration, 0.3Hz. Preparations were fixed and processed immediately after fill. Neurobiotin was visualized by addition of Streptavidin conjugated to Alexa Fluor dyes (1:500; Molecular Probes) during the incubation step with secondary antibodies.

Backfills

For nerve backfills, a Vaseline well was built around the nerve and the well was filled with diH_2O for five minutes. Then the water was replaced with one of the following tracers: 6% rhodamine- or fluorescein-dextran-10 kDa (Molecular Probes) or 4% neurobiotin tracer (Vector Laboratories) in 50mM Tris buffer and 0.5M KCl, or with 100mM Lucifer Yellow-CH Lithium salt (Molecular Probes). The nerve was cut inside the well, and the preparations were incubated for 16 hours at 12° C or for 48 hours at 4° C with daily saline changes, after which the Vaseline well was removed and the preparations were fixed and processed.

Neurobiotin was visualized by addition of Streptavidin conjugated to Alexa Fluor dyes (1:500; Molecular Probes) during the incubation step with secondary antibodies.

Image acquisition and processing

Standard fluorescent images were taken on an IX81 Motorized Inverted Scope (Olympus) using Volocity software Version 4.3.2 Build 23 (Improvision, Perkin-Elmer). Confocal images were collected on either a Leica SP2 or SP5 CLEM microscope using Leica Application Suite Advanced Fluorescence (LAS AF) software 2.1.0 Build 4316. Image stacks were converted to .ims files with Imaris 7.0 - 7.2 (Bitplane). The Imaris Slice and Surpass modules were used for adjusting contrast and brightness and to display stacks as maximum intensity projections (Figs. 3 and 8) or in gallery view (Fig.6), and snapshots were exported as .tif files for final figure assembly in Illustrator CS4 (Adobe Systems). For figures 2, 4 and 5, images were imported into Image J (NIH), point-spread functions (PSF) were calculated using the Diffraction PSF 3D plugin, and images were converted to 16-bit grayscale using the Parallel Spectral Deconvolution 2D plugin, Version 1.7 and finally edited for brightness and / or contrast using Photoshop CS5 (AdobeSystems). Images for Figure 7 were traced, digitized and edited using Canvas 10.0 (ACD Systems). Traces for Figure 9A were recorded using Clampex 10.0 (Molecular Devices) and arranged using Adobe Illustrator CS5 (Adobe Systems). The plot in Figure 9B was created using Microsoft Excel, and Figure 9 was completed in Canvas 10.0 (ACD Systems).

Direct tissue analysis

All animals were anesthetized by packing in ice for 30-60 minutes (n = 6), after which the STNS was dissected from surrounding tissues in chilled physiological saline (~10°C), and the sheath surrounding the ganglia was completely removed on both sides. Direct tissue analysis was performed as described previously (Kutz et al., 2004). Briefly, the tissue was rinsed in a droplet of acidified methanol (90% methanol: 9% glacial acetic acid: 1% deionized water), desalted in a droplet of dilute MALDI matrix (10 mg/ml 2, 5-dihydroxybenzoic acid (DHB), aqueous), and placed on the MALDI plate. 0.4 μL DHB (50 mg/ml in 50% methanol, v/v) matrix was deposited on top of the tissue to adhere it to the MALDI target and allowed to crystallize at room temperature. Direct tissue mass spectrometric analysis was performed using MALDI TOF/TOF.

MALDI TOF/TOF

A model 4800 MALDI TOF/TOF analyzer (Applied Biosystems, Framingham, MA) equipped with a 200 Hz, 355 nm Nd:YAG laser (spot diameter of 75μm) was used for all mass spectral analyses. Acquisitions were performed in positive ion reflectron mode. Instrument parameters were set using the 4000 Series Explorer Software (Applied Biosystems). Mass spectra were externally calibrated using peptide standards applied directly to the stainless steel MALDI target. Tandem mass spectra (MS/MS) were achieved by 2 kV collision induced dissociation (CID) using air as the collision gas. 750 laser shots were averaged for each MS/MS spectrum, and sequence interpretation was performed manually.

Electrophysiological experiments

Recordings from the STG and its nerves were performed as previously described (Goaillard et al., 2004). Stainless steel pins were connected to an A-M Systems Inc. amplifier (Carlsborg, WA) and placed in Vaseline wells surrounding the lateral ventricular nerve (*lvn*) to obtain extracellular recordings from axons of the pyloric network motor neurons: the Pyloric (PY), Lateral Pyloric (LP), and Pyloric Dilator (PD) neurons. Intracellular recordings from somata in the STG were made using sharp electrodes (15–25 MΩ, filled

with 0.6 M K_2SO_4 and 20 mM KCl) and Brownlee (Automate Scientific, Inc., Berkeley, CA) and Axoclamp 2B (Molecular Devices, Sunnyvale, CA) amplifiers. Data were collected using Clampex 10.0 (Molecular Devices) software. All B-type allatostatin peptides were synthesized at the University of Wisconsin unless otherwise stated.

During experiments preparations were superfused continuously with *C. borealis* saline (~10 ml/min) and temperature was maintained at 10–12°C using a Peltier (Warner Instruments, Hamden, CT). Spike 2, version 6.04, (Science Products GmbH, Hofheim, Germany), Clampfit 10.0 (Molecular Devices) and Excel (Microsoft) were used for data analysis.

Results

Identification of B-type AST peptides in the STNS using MALDI TOF/TOF

A large number of previously reported neuropeptides were observed in the STNS, including the STG and CoG (Fig. 1A, B) using direct tissue mass spectrometric analysis. Many of these peptides belong to well-known neuropeptide families, such as the RFamides and orcokinins, among many others. Multiple members of the B-type ASTs were present, although they were represented by peaks with relatively lower intensities in the spectra (Fig. 1A, denoted by squares). Mass spectrometry also detected B-type ASTs in the stomatogastric nerve (*stn*) and superior esophogeal nerve (*son*), which connect the STG with the OG and CoGs. No B-ASTs were found in the inferior oesophageal nerve (*ion*) or the dorsal ventricular nerve (*dvn*). Tandem mass experiments were performed directly on the tissue samples to confirm the identities of the observed peptide peaks. As shown in the example in Figure 1C, many immonium ions and several sequence related b and y ions were observed in the collisional-induced dissociation (CID) fragmentation analysis of the B-type AST SGKWSNLRGAWamide (B3; m/z 1260.7).

Six preparations were analyzed using direct tissue mass spectrometric techniques, and each preparation was analyzed three times on MALDI TOF/TOF to eliminate random errors of detection. The B-type allatostatins detected are shown in Table 2. In total, nine different isoforms were found to be present in the STG, CoG and *stn* including: CbAST-B1 (VPNDWAHFRGSWa), CbAST-B2 (QWSSMRGAWa), CbAST-B3 (SGKWSNLRGAWa), CbAST-B4 (NWNKFQGSWa), CbAST-B5 (TSWGKFQGSWa), CbAST-B6 (GNWNKFQGSWa), CbAST-B7 (NNWSKFQGSWa), CbAST-B8 (STNWSSLRSAWa), and CbAST-B9 (NNNWSKFQGSWa).

Characterization of B-type AST staining in the STNS of *C. borealis*

A-, B- and C-type allatostatins inhibit the pyloric rhythm in the STG (Fu et al., 2007; Ma et al., 2009b; Skiebe and Schneider, 1994). The distribution of A-type ASTs has been well-characterized in the STNS of several crustaceans (Skiebe, 1999; Skiebe and Schneider, 1994), but the distribution of B-type ASTs in the STNS has not yet been described. Using an antibody raised against the B-type allatostatin VPNDWAHFRGSW-amide (CbAST-B1; see Methods), we determined the distribution of CbAST-B1-like immunoreactivity (CbAST-B1-LI) in the STNS of *C. borealis* (n=26).

The CoGs

The two CoGs each contain ~400- 500 somata and a large neuropil (Coleman et al., 1992). In the CoGs, the CbAST-B1 antibody stained both the neuropil and cell bodies (Fig. 2). About 30-40 cells ranging from 15 to 30μm in size stained brightly in each CoG (n=32 ganglia). 1-2 large cells with diameters of 40-50 μm were also sometimes apparent. Figure 2A shows a low magnification view of CbAST-B1-LI in the entire CoG, and Figure 2B shows a section midway through the same ganglion to show the immunoreactive fibers

connecting the circumoesophageal connective (CoC) to the neuropil of the CoG (white asterisk). In this preparation three brightly immunostained fibers made this characteristic turn into the CoG. In different preparations the number of discernable fibers varied from 1-4, and Figure 2C shows an example of another preparation where two of these fibers and their arborizations were evident. A large CoC fiber bundle also extended between the brain and the CoG neuropil (Fig. 2B double arrows). CbAST-B1-LI was also apparent in fibers traveling in the CoC between the brain and thoracic ganglion directly (Fig. 2B, arrowheads).

An examination of the nerves connecting the CoGs with other STNS ganglia demonstrated 1-4 brightly labeled fibers in the *son* (n=15), (Fig. 2B) that could be traced from the CoGs to the *stn*. Some of these fibers also extended into the dorsal posterior esophageal nerve (*dpon*). In the portion of the *son* proximal to the CoG, 1-4 small somata were apparent in 10 out of 14 preparations (Fig. 2A, box, Fig. 2D). The *son* also revealed punctate labeling throughout the length of the nerve. In addition, 1-2 faintly stained fibers were sometimes seen in the *ions* (Fig. 2B, top white arrow), although this labeling was not as prominent as the *son* labeling.

The OG

In *C. borealis*, the OG contains ~ 14 somata (Coleman et al., 1992). Three of these neurons extend processes into the *stn*: the two Modulatory Proctolin Neurons (MPNs) (Nusbaum and Marder, 1989a; Nusbaum and Marder, 1989b) and the Cardiac Sac Dilator Neuron 1 (CD1) (Vedel and Moulins, 1977). We combined back-fills of various nerves with CbAST-B1-LI to determine which of the OG somata showed CbAST-B-LI (n = 3 for *stn* backfills, n=3 for *ion* backfills, n=2 for *son* backfills).

Figure 3 shows OGs from two different preparations labeled for CbAST-B-LI. Note that there are 4 brightly stained somata, and another 6-7 moderately to weakly stained somata. In 11 immunostained OGs, the number of somata varied from three to as many as eleven in the example shown in Figure 3A. Note also in Figure 3A that clearly stained fibers in the *on* and in the *ion* are seen, while a different preparation (Fig. 3B) shows only 6 distinctly labeled somata and no fibers in the adjacent nerves. Figure 3C shows the results of the dye backfill from the *stn* for the same preparation as in Figure 3A. At least 5-6 stained fibers are seen in the *on*, and the two smaller, MPN neurons and the large, CD1 neuronal somata are brightly labeled. Additionally, fibers project into the *ion* and *ivn*. Figure 3C shows the merge of these two images, showing that the MPNs exhibited intense CbAST-B1-LI and the CD1 neuron was less intensely stained. Figure 3D also shows a number of neurons that exhibited strong CbAST-B1-LI, but were not labeled by the *stn* backfill.

Backfills from a single *ion* labeled 4 somata, as shown in Figure 3E. Of these, one small neuron showed bright and one large neuron showed weak CbAST-B1-LI (Figure 3F). Double label experiments showed that the single CabTRP1a-staining neuron (Blitz et al., 1995; Christie et al., 1997; Goldberg et al., 1988) with *ion* projections is also immunoreactive for CbAST-B1 (data not shown).

The stn-on-son junction

The *stn* is the only nerve connecting the STG with the anterior ganglia (CoGs and OG) which provide descending modulatory inputs to the pyloric and gastric networks in the STG. Coleman et al (1992) found ~ 55-60 medium to large diameter fibers in the *stn*. In addition to axons from the three neurons in the OG that project to the STG, ~20 pairs of CoG somata project to the *stn* via the *sons* (Coleman et al., 1992). Additionally, up to 10 *stn* fibers originate from neurons in the STG (Goldberg et al., 1988). In 18 preparations, 4 to 9 CbAST-B1-LI fibers were seen in the *stn*. Of those, one to four fibers could be traced from

punctate staining in the *son* to the anterior *stn* neuropil and along the *stn* (n=15). Punctate staining in the anterior *stn* was abundant and large and small varicosities were present at various sites in the *stn* (Figure 4A, arrow; Figure 4B).

STG

The STG of *C. borealis* contains approximately 25-26 neurons (Kilman and Marder, 1996). None of the STG somata showed CbAST-B1-LI. However, the STG neuropil, which is surrounded by these somata, was brightly stained and the stained fibers were distributed diffusely in this region (Fig. 5). CbAST-LI fibers that projected into the STG neuropil from the *stn* appeared to be located mostly on one side of this nerve (Fig. 5, arrow; n=20). Both fine fibers and bulbous swellings up to ~10 μm in size were apparent in the neuropil (Fig. 5, arrowhead). In addition, immunoreactive fibers usually extended posteriorly 50-100 μm from the neuropil into the *dvn* (Fig. 5, double arrows). It was previously shown that most peptide immunostaining in the STG is localized to the periphery of the neuropil where fine processes and branches are numerous, while the center of the neuropil is occupied by the large primary neurites (Baldwin and Graubard, 1995; Kilman and Marder, 1996). CbAST-B1-LI demonstrated a similar pattern of distribution (n=30; Fig. 6). Extensive staining was apparent as a rind around the outside of the neuropil, but was sparse in the center where the largest neuronal processes are present.

CbAST-B1-LI in the posterior STNS (the region containing axonal processes of STG motor neurons) was rarely seen. In a few preparations, a single small fiber posterior to the STG in the *dvn* and *lvn* was stained. This is consistent with the fact that some neurons projecting from the CoGs and OG send processes through the STG and into the *dvn* and *lvn* (Coleman et al., 1992). Occasional bright spots of punctate staining were seen in the *dvn* and *lvn*. The gastro-pyloric receptor (GPR) cells, which contain serotonin and acetylcholine (Katz et al., 1989; Katz and Harris-Warrick, 1989) and send processes through the *lvn* and *dvn* to the STG were not immunoreactive for CbAST-B1.

A summary of CbAST-B1 antibody staining in the STNS of the crab, *C. borealis* is shown in Figure 7.

Specificity controls

Given the presence of at least 9 different isoforms of CbAST-B (Table 1), it was important to determine whether this antibody is likely to recognize all of these peptides, or only the isoform to which it was raised. Consequently, CbAST-B1 antibodies were preincubated with the CbAST-B1 peptide (sequence VPNDWAHFRGSW-amide) at varying concentrations (n=30). Staining was abolished by preincubation with CbAST-B1 at concentrations of 10^{-6} M and higher. Weak staining was observed when the antibody was preincubated with 10^{-7} M CbAST-B1, and the staining increased in intensity until it reached control levels following preincubation with 10^{-9} M CbAST-B1 peptide (data not shown).

Preincubations with two additional B-type ASTs indicated that the antibody is likely to recognize other CbAST-B peptides, albeit to a lesser degree. Preincubation with 10^{-4} M CbAST-B2 (QWSSMRGAW-amide; n=9) and 10^{-4} M CbAST-B3 (SGKWSNLRGAW-amide; n=7) only partially blocked staining in the STG, but staining in the CoGs was almost completely blocked.

Comparison of CbAST-A and CbAST-B-LI in the STNS

The distribution of AST A-like immunoreactivity in the STNS of various crustacean species has been previously characterized (Skiebe, 1999; Skiebe and Schneider, 1994). To determine whether the distribution of B-type ASTs is likely to be similar to that of the A-

types, we examined the distribution of A- and B-type immunoreactivity in the same preparations. Many of the descending modulatory projection neurons in the STNS colocalize multiple transmitters (Blitz et al., 1999; Blitz and Nusbaum, 1999; Kilman et al., 1999; Nusbaum, 2002; Nusbaum and Beenhakker, 2002; Nusbaum et al., 2001; Thirumalai and Marder, 2002). In examining the distribution of both ASTs, we also wanted to determine whether any of the same neurons colocalized members of the two peptide families. These studies were performed using the CbAST-B1 antibody as well as antibodies raised against a cockroach A-type AST (Dippu-AST-7), which possess the same carboxy terminal sequence as A-type ASTs in crustaceans (Ma et al., 2009c). The CbAST-B1 antiserum was raised in rabbit and the Dippu-AST7 antibody is a mouse monoclonal, which aided in obtaining distinctive double-labeling.

Preparations were simultaneously exposed to both the CbAST-B1 antibody (Fig. 8A) as well as antibodies against Dippu-AST-7, (Fig. 8B; n=11). In general, most cells and cellular processes that were immunoreactive to the CbAST-B1 antibody were not stained by the AST-A antibody. In the CoGs, AST-A-like staining was also seen in both the neuropil and cell bodies (Fig. 8B). Neuropil fibers that exhibited CbAST-A-LI were not the same as those exhibiting CbAST-B-LI. This was determined by an examination of both the 3D projection images as well as a slice by slice comparison of fluorescently stained fibers. In addition, A-type neuropil staining was located more centrally (Fig. 8C). In all preparations, two large neurons (~ 60μm) were lightly but consistently stained using the Dippu-AST 7 antibody, but not the CbAST-B1 antibody (Fig. 2C, 2D). These cells were much larger than the cells that typically stained brightly with the CbAST-B1 antibody. A subset of small cells showed bright CbAST-B1-LI and weak Dippu-AST-7-like immunoreactivity (Fig. 8D). Using a different AST-A antibody, Skiebe and Schneider (1994) also saw two large cells and ~12-19 smaller cells in the CoG, including ~8 medium (15-25μm) and up to nine smaller (5-10μm) cell bodies. In our experiments, somata with a small diameter (~20μm) that were stained by the Dippu-AST-7 antibody were apparent in two preparations. These cells were similar in size to those stained by the CbAST-B1 AST antibody.

AST-A immunoreactive somata were not apparent in the OG. However, there were AST-A-LI fibers in the *son* that did not co-localize with those stained by the CbAST-B1 AST antibody (data not shown). Typically, only one to two fibers that stained for AST-A entered the STG from the *stn*, compared to the 3-4 CbAST-B1-like immunoreactive fibers (Fig. 8E). At this site, fibers stained with the two antibodies were clearly distinct with no overlap in the *stn*. In the STG, both antibodies extensively stained processes in the neuropil; somatic staining was never apparent (n=8).

One major difference between the CbAST-B-type staining and that previously described for the A-type ASTs is in the region of the STNS posterior to the STG. As previously discussed, B-type fiber staining was rarely observed in this region, while extensive A-type staining was previously described (Skiebe and Schneider, 1994). In particular, A-type AST-like immunoreactivity is seen in the GPR cells, stretch receptor cells that play an important roles in modulating gastric and pyloric rhythms (Beenhakker et al., 2005; Katz et al., 1989; Katz and Harris-Warrick, 1989). In contrast, these cells exhibited no CbAST-B1-LI. CbAST-A immunoreactive fibers were also consistently observed extending past the STG neuropil into the *dvn* and posterior STNS (data not shown).

To determine whether there was any cross-reactivity between the CbAST-B1 antibody and A-type ASTs, CbAST-B1 antibodies were preincubated with 10^{-4}M Dippu-AST-3. These preincubation experiments resulted in STNS staining identical to controls (n=4; data not shown). Thus, as predicted from the fact that there is no sequence homology between the three AST families, A-type ASTs are apparently not detected by the CbAST-B1 antiserum.

Physiological effects of CbAST-B peptides on the pyloric rhythm

Individual members of the A, B, and C AST families of peptides inhibit the pyloric rhythm in a state-dependent manner (Fu et al., 2007; Ma et al., 2009b; Skiebe and Schneider, 1994). This previous work studied the effects of several insect AST-A peptides, CbAST-B1 and the two C-type CbAST peptides and found that preparations with strong initial frequencies (~1Hz) were less inhibited by peptide applications while preparations with initial pyloric burst frequency less than ~0.5 Hz, were silenced by peptide applications.

To determine whether CbAST-B2 and CbAST-B3 exerted similar effects on the pyloric rhythm as CbAST-B1, we applied these peptides to the STG (n=22). Figure 9A shows recordings from a single preparation and illustrates that high concentrations of each of these peptides completely inhibited the pyloric rhythm. At 10^{-5} M all three peptides silenced the pyloric rhythm, and these effects were readily reversible (Fig. 9A). Note that in the absence of IPSPs the LP neuron's membrane potential hyperpolarized in the presence of the peptides, and that in addition to the LP neuron, the PD and PY neurons (also seen on the *lvn* recording) were silenced.

Figure 9B compares the effects of application of 10^{-8}M CbAST-B1, CbAST-B2, and CbAST-B3 on the pyloric rhythm. Examination of the plot shows evidence of state-dependence, in which faster initial baseline frequencies showed little decrease in frequency in peptide, whereas slower initial baseline frequencies exhibited greater decreases in frequency. To quantify these results, we rank-ordered all of the data by initial frequency, and then cut the population in two bins, above and below the median burst frequency of 0.64 Hz. The high initial frequency group (n =19) decreased 11.1% in 10^{-8} M peptide, while the low initial frequency group (n= 18) decreased 52.6% in 10^{-8} M peptide. These values are significantly different (Mann-Whitney Rank Sum Test, p = 0.002).

The state-dependent action of these peptides makes preparation to preparation comparisons of dose-response curves difficult unless all of the studied preparations are from a population of similar starting frequencies. Nonetheless, previous studies estimated the EC50 for CbAST-B1 peptide at ~10^{-8} M (Fu et al., 2007). We obtained similar data in dose-response experiments for CbAST-B2 and CbAST-B3 peptides. To remove the influence of the initial frequency on a potential comparison of the actions of CbAST-B2 and CbAST-B3, we compared data from preparations with initial frequencies of between 0.5 and 0.67 Hz. 10^{-8} M CbAST-B2 decreased the pyloric rhythm frequency by 44% (n =6) and 10^{-8} M CbAST-B3 decreased the frequency by 37% (n = 6). These values were not statistically different (Student's T-test, p = 0.643).

Discussion

Peptides play a variety of important roles in reconfiguring the circuits that control behavior in all animals (Marder and Bucher, 2007; Marder and Calabrese, 1996). Some peptides reach their targets via release from neurons with well-defined projections (Nusbaum, 2002; Nusbaum et al., 2001), while other peptides reach their targets via the hemolymph (Christie et al., 1995). One of the salient findings from decades of work on the modulation of the crustacean STG is that the STG motor patterns are modulated by a very large number of amines and neuropeptides (Marder and Bucher, 2007; Marder and Calabrese, 1996). Moreover, at least 142 different neuropeptides, members of at least 17 different peptide families were found in *C. borealis* (Ma et al., 2009c), many of them in the stomatogastric nervous system. Several questions immediately arise: a) Are there significant differences in the physiological actions of different members of the same peptide family? b) Are different members of the same peptide family differentially distributed in the nervous system? c) What are the complete patterns of colocalization of peptides of the same family and of

different families? The eventual answers to these questions will require many studies combining immunocytochemistry, mass spectrometry, and electrophysiology. The results in this paper on the CbAST-B family of peptides are both interesting in their own right and part of this larger effort.

Previous work had described 10 different members of the AST-B family that were identified in *C. borealis* tissues including the brain, pericardial organs, and sinus glands, as well as the ganglia of the STNS (Ma et al., 2009c). Nonetheless, the methods of the previous paper were of insufficient resolution to find most of the *C. borealis* AST-B peptides in the STNS. In this paper, we detected nine of these previously identified CbAST-Bs and described their anatomical localization throughout the STNS. Many of these peptides were at low abundance and were seen only after the sensitivity of direct tissue mass spectral detection of neuropeptides was improved by physically removing the sheath surrounding the ganglia and nerves in the STNS, permitting more efficient extraction of neuropeptide inside the tissue into the MALDI matrix solution enabling peptide profiling. It is hard to interpret the low abundance of these peptides in extracts of the STNS, because it is not clear how many of the different isoforms are found in the same neurons, and whether they are coreleased. Given that the physiological actions of the three CbAST-Bs we studied were so similar, it is possible that the low abundance of any single peptide may be compensated for by the corelease of a number of the isoforms from the same neurons.

As previously discussed, the nomenclature of the inhibitory peptides termed “allatostatins” is misleading. Although the three allatostatin families were so named on the basis of their activity in the insects in which they were discovered, the AST-A, AST-B and AST-C peptides are not structurally related. In recent years it has become clear that the three groups of peptides are encoded on different genes, and act on distinct receptors (Hauser et al., 2006). AST-A, -B, and -C receptors are G-protein coupled receptors (GPCRs) related to 3 vertebrate receptor groups: galanin (Kastin, 2006), bombesin (Johnson et al., 2003), and somatostatin (Veenstra, 2009), respectively. In addition, the AST-B (MIP) receptor has been tentatively identified only in *Drosophila* (Johnson et al., 2003), where it has been shown to activate the sex peptide receptor (Kim et al., 2010). Also, in *Drosophila*, AST-Bs (MIPs) are part of a peptide signaling cascade involved in the regulation of ecdysis (Kim et al., 2010), which might have implications for the modulation of motor rhythms in the STG.

Many peptide families in *C. borealis* have a large number of isoforms, including the FMRFamide-related peptides (FaRPs), AST-A's, orcokinins, and CabTRPs (Ma et al., 2009c; Stemmler et al., 2009). In some cases, the affinity of these variants for their receptors may vary (Skiebe and Schneider, 1994), while in other cases, there may be relatively little difference when they are bath-applied under usual *in vitro* conditions, but different isoforms may have different stability or resistance to peptidases, and therefore may be preferentially active under a given set of physiological conditions (Cruz-Bermudez et al., 2006).

To the best of our knowledge, the antibody reported here is the first raised against any of the crustacean AST-Bs. Because of the extensive sequence homology of the CbAST-Bs, we assume that this antiserum recognizes all members of this family, albeit with different affinity. The tissue blocks we performed establish that the antibody has a higher affinity for CbAST-B1 than for CbAST-B2 and CbAST-B3. Nonetheless, without knowing the relative concentrations of the isoforms in the stained tissue, we can only say that the antibody is labeling one or more of the CbAST-B family of peptides, and more specific determination of the relevant distribution of the different isoforms will require high-resolution MALDI imaging (Chen et al., 2009; DeKeyser et al., 2007). Likewise, although the AST-A antibody we used is monoclonal (Stay et al., 1992), we assume that it is likely to have a higher affinity to the CbAST-As that have the closest homology to the peptide against which it was

raised (Stay et al., 1992), but that it may also label any of the almost 40 members of the CbAST-A family of peptides (Ma et al., 2009c).

The double-label experiments shown here suggest relatively little colocalization between the AST-A and AST-B families in the STNS of *C. borealis*, despite the fact that these classes of peptides, along with the AST-Cs, show superficial similarities in their physiological actions (Fu et al., 2007; Ma et al., 2009b; Skiebe and Schneider, 1994). The three AST families have no structural similarity, and in insects are known to activate different classes of GPCRs, each with homologies to different families of vertebrate receptors (Birgul et al., 1999; Mayoral et al., 2010; Stay and Tobe, 2007). What we do not yet know is whether these three peptide classes are acting on the same target neurons, or whether the superficial similarity in these physiological actions results from different circuit mechanisms. In contrast, the terminal sequence of the three forms of the CbAST-Bs studied here are structurally very similar, and they showed similar dose-response curves, strongly suggesting that the CbAST-B receptor does not distinguish among these peptides.

The MPNs are a pair of neurons in the OG that contain proctolin and GABA (Blitz et al., 1999; Blitz and Nusbaum, 1999) and are important regulators of the STG motor patterns. We now add a third cotransmitter to the complement found in the MPNs. On some of the MPN target neurons, the effects of CbAST-B peptides and GABA might be synergistic. If the CbAST-B peptides act directly on the same neurons that respond strongly to proctolin, these substances could well be acting in seeming opposition, as proctolin is strongly excitatory on all of its known targets (Golowasch and Marder, 1992; Swensen and Marder, 2000; 2001). Equally interesting will be assessment of the potential actions of the CbAST-B peptides in CD1. CD1 is a cholinergic excitatory motor neuron that innervates several cardiac sac muscles, and it will be interesting to see if its neuromuscular junctions are modulated by this new peptide cotransmitter.

The CbAST-B family joins a large number of other neuromodulatory substances that show punctate staining in the *stn* (Callaway et al., 1987; Kilman et al., 1999; Marder et al., 1987; Marder et al., 1986; Mortin and Marder, 1991), in the same vicinity where synaptic contacts are seen (Goaillard et al., 2004; Skiebe and Ganeshina, 2000; Skiebe and Wollenschlager, 2002). The localization of CbAST-B family peptides at this site suggests that these peptides might influence information flow between the anterior ganglia of the STNS and the STG.

One of the most unusual features of the actions of all three families of the CbASTs is their state-dependence. Because these peptides are more effectively inhibitory when the pyloric rhythm is relatively weak, the CbAST-B state-dependence might be seen as a positive feedback that amplifies any other factors that tend to decrease the excitability of the network. On the other hand, the action of CbAST-B family peptides that are released as a consequence of MPN activity will be potentially accompanied by proctolin, which would tend to maintain the excitability of the preparation, thus diminishing the potential action of the CbAST-B-family of peptides. Interestingly, the excitatory actions of proctolin are also state-dependent, and proctolin is also more effective when applied to preparations that show slow pyloric rhythms (Nusbaum and Marder, 1989b). Thus, the state-dependence of the proctolin excitatory actions and the inhibitory CbAST-B peptides may be well-balanced to maintain overall MPN action.

Given that the three AST peptide families are not structurally related and are encoded by different genes, it is remarkable that they share two seemingly unrelated properties. Not only have all ASTs first been identified from insects by their inhibitory action on hormone synthesis and secretion, but they also happen to be the only neuropeptides described to date that inhibit STNS activity. Indeed, the only other known inhibitory transmitters/modulators

in this system are GABA (Cazalets et al., 1987; Swensen et al., 2000)and histamine (Christie et al., 2004; Claiborne and Selverston, 1984). Because the crustacean stomach is shed during molting, and therefore the STG motor patterns are inhibited before molting (Clemens et al., 1999), it is possible that there are shared evolutionary pressures that result in the shared use of these three peptide families to be also employed to inhibit feeding-related network activity during molting.

Acknowledgments

The AST-A monoclonal antibody used in this study was obtained from the Developmental Studies Hybridoma Bank developed under the auspices of the NICHD and maintained by The University of Iowa, Department of Biology, Iowa City, IA 52242. We thank Mr. Ed Dougherty for help with the confocal microscopes, and Drs. Adam Taylor and Ted Brookings for useful discussions.

Research supported by NS 17813 (EM, TMS), P01 NS044232 (LT), T32 NS 007292 (MG), DK 071801 (LL).

References

Audsley N, Matthews HJ, Price NR, Weaver RJ. Allatoregulatory peptides in Lepidoptera, structures, distribution and functions. J Insect Physiol. 2008; 54(6):969–980. [PubMed: 18377924]

Audsley N, Weaver RJ. Identification of neuropeptides from brains of larval Manduca sexta and Lacanobia oleracea using MALDI-TOF mass spectrometry and post-source decay. Peptides. 2003; 24(10):1465–1474. [PubMed: 14706525]

Audsley N, Weaver RJ. Neuropeptides associated with the regulation of feeding in insects. Gen Comp Endocrinol. 2009; 162(1):93–104. [PubMed: 18775723]

Baldwin DH, Graubard K. Distribution of fine neurites of stomatogastric neurons of the crab, *Cancer borealis*: evidence for a structured neuropil. J Comp Neurol. 1995; 356:355–367. [PubMed: 7642799]

Beenhakker MP, DeLong ND, Saideman SR, Nadim F, Nusbaum MP. Proprioceptor regulation of motor circuit activity by presynaptic inhibition of a modulatory projection neuron. J Neurosci. 2005; 25(38):8794–8806. [PubMed: 16177049]

Bendena WG, Donly BC, Tobe SS. Allatostatins: a growing family of neuropeptides with structural and functional diversity. Ann N Y Acad Sci. 1999; 897:311–329. [PubMed: 10676459]

Birgul N, Weise C, Kreienkamp HJ, Richter D. Reverse physiology in drosophila: identification of a novel allatostatin-like neuropeptide and its cognate receptor structurally related to the mammalian somatostatin/galanin/opioid receptor family. EMBO J. 1999; 18(21):5892–5900. [PubMed: 10545101]

Blitz DM, Christie AE, Coleman MJ, Norris BJ, Marder E, Nusbaum MP. Different proctolin neurons elicit distinct motor patterns from a multifunctional neuronal network. J Neurosci. 1999; 19:5449–5463. [PubMed: 10377354]

Blitz DM, Christie AE, Marder E, Nusbaum MP. Distribution and effects of tachykinin-like peptides in the stomatogastric nervous system of the crab, *Cancer borealis*. J Comp Neurol. 1995; 354:282–294. [PubMed: 7782503]

Blitz DM, Nusbaum MP. Distinct functions for cotransmitters mediating motor pattern selection. J Neurosci. 1999; 19:6774–6783. [PubMed: 10436035]

Boonen K, Landuyt B, Baggerman G, Husson SJ, Huybrechts J, Schoofs L. Peptidomics: the integrated approach of MS, hyphenated techniques and bioinformatics for neuropeptide analysis. Journal of separation science. 2008; 31(3):427–445. [PubMed: 18266258]

Callaway JC, Masinovsky B, Graubard K. Co-localization of SCPB-like and FMRFamide-like immunoreactivities in crustacean nervous systems. Brain Res. 1987; 405(2):295–304. [PubMed: 3567607]

Cazalets JR, Cournil I, Geffard M, Moulins M. Suppression of oscillatory activity in crustacean pyloric neurons: Implication of GABAergic inputs. J Neurosci. 1987; 7:2884–2893. [PubMed: 3625277]

Chen R, Hui L, Sturm RM, Li L. Three Dimensional Mapping of Neuropeptides and Lipids in Crustacean Brain by Mass Spectral Imaging. J Am Soc Mass Spectrom. 2009

Chen R, Jiang X, Conaway MC, Mohtashemi I, Hui L, Viner R, Li L. Mass spectral analysis of neuropeptide expression and distribution in the nervous system of the lobster Homarus americanus. Journal of proteome research. 2010; 9(2):818–832. [PubMed: 20025296]

Christie AE, Cashman CR, Brennan HR, Ma M, Sousa GL, Li L, Stemmler EA, Dickinson PS. Identification of putative crustacean neuropeptides using in silico analyses of publicly accessible expressed sequence tags. General and comparative endocrinology. 2008; 156(2):246–264. [PubMed: 18321503]

Christie AE, Lundquist T, Nässel DR, Nusbaum MP. Two novel tachykinin-related peptides from the nervous system of the crab *Cancer borealis*. J Exp Biol. 1997; 200:2279–2294. [PubMed: 9316266]

Christie AE, Skiebe P, Marder E. Matrix of neuromodulators in neurosecretory structures of the crab, *Cancer borealis*. J Exp Biol. 1995; 198:2431–2439. [PubMed: 8576680]

Christie AE, Stein W, Quinlan JE, Beenhakker MP, Marder E, Nusbaum MP. Actions of a histaminergic/peptidergic projection neuron on rhythmic motor patterns in the stomatogastric nervous system of the crab *Cancer borealis*. J Comp Neurol. 2004; 469(2):153–169. [PubMed: 14694531]

Christie AE, Stemmler EA, Dickinson PS. Crustacean neuropeptides. Cell Mol Life Sci. 2010; 67(24): 4135–4169. [PubMed: 20725764]

Claiborne B, Selverston A. Histamine as a neurotransmitter in the stomatogastric nervous system of the spiny lobster. J Neurosci. 1984; 4:708–721. [PubMed: 6142932]

Clemens S, Massabuau JC, Meyrand P, Simmers J. Changes in motor network expression related to moulting behaviour in lobster: role of moult-induced deep hypoxia. J Exp Biol. 1999; 202:817–827. [PubMed: 10069971]

Clynen E, Liu F, Husson SJ, Landuyt B, Hayakawa E, Baggerman G, Wets G, Schoofs L. Bioinformatic approaches to the identification of novel neuropeptide precursors. Methods in molecular biology (Clifton, NJ. 2010; 615:357–374.

Coleman MJ, Nusbaum MP, Cournil I, Claiborne BJ. Distribution of modulatory inputs to the stomatogastric ganglion of the crab, *Cancer borealis*. J Comp Neurol. 1992; 325:581–594. [PubMed: 1361498]

Cruz-Bermudez ND, Fu Q, Kutz-Naber KK, Christie AE, Li L, Marder E. Mass spectrometric characterization and physiological actions of GAHKNYLRFamide, a novel FMRFamide-like peptide from crabs of the genus *Cancer*. J Neurochem. 2006; 97(3):784–799. [PubMed: 16515542]

Cruz-Bermudez ND, Marder E. Multiple modulators act on the cardiac ganglion of the crab, Cancer borealis. J Exp Biol. 2007; 210(Pt 16):2873–2884. [PubMed: 17690236]

Cuello AC, Galfre G, Milstein C. Detection of substance P in the central nervous system by a monoclonal antibody. Proc Natl Acad Sci U S A. 1979; 76(7):3532–3536. [PubMed: 386341]

DeKeyser SS, Kutz-Naber KK, Schmidt JJ, Barrett-Wilt GA, Li L. Imaging mass spectrometry of neuropeptides in decapod crustacean neuronal tissues. Journal of proteome research. 2007; 6(5): 1782–1791. [PubMed: 17381149]

Dickinson PS, Stemmler EA, Barton EE, Cashman CR, Gardner NP, Rus S, Brennan HR, McClintock TS, Christie AE. Molecular, mass spectral, and physiological analyses of orcokinins and orcokinin precursor-related peptides in the lobster *Homarus americanus* and the crayfish *Procambarus clarkii*. Peptides. 2009a; 30(2):297–317. [PubMed: 19007832]

Dickinson PS, Wiwatpanit T, Gabranski ER, Ackerman RJ, Stevens JS, Cashman CR, Stemmler EA, Christie AE. Identification of SYWKQCAFNAVSCFamide: a broadly conserved crustacean C-type allatostatin-like peptide with both neuromodulatory and cardioactive properties. J Exp Biol. 2009b; 212(Pt 8):1140–1152. [PubMed: 19423507]

Dircksen H, Skiebe P, Abel B, Agricola H, Buchner K, Muren JE, Nassel DR. Structure, distribution, and biological activity of novel members of the allatostatin family in the crayfish Orconectes limosus. Peptides. 1999; 20(6):695–712. [PubMed: 10477125]

Duve H, Johnsen AH, Maestro JL, Scott AG, Jaros PP, Thorpe A. Isolation and identification of multiple neuropeptides of the allatostatin superfamily in the shore crab *Carcinus maenas*. Eur J Biochem. 1997; 250(3):727–734. [PubMed: 9461295]

Duve H, Johnsen AH, Scott AG, Thorpe A. Allatostatins of the tiger prawn, *Penaeus monodon* (Crustacea: Penaeidea). Peptides. 2002; 23(6):1039–1051. [PubMed: 12126730]

Fu Q, Goy MF, Li L. Identification of neuropeptides from the decapod crustacean sinus glands using nanoscale liquid chromatography tandem mass spectrometry. Biochem Biophys Res Commun. 2005a; 337(3):765–778. [PubMed: 16214114]

Fu Q, Kutz KK, Schmidt JJ, Hsu YW, Messinger DI, Cain SD, de la Iglesia HO, Christie AE, Li L. Hormone complement of the *Cancer productus* sinus gland and pericardial organ: an anatomical and mass spectrometric investigation. J Comp Neurol. 2005b; 493(4):607–626. [PubMed: 16304631]

Fu Q, Tang LS, Marder E, Li L. Mass spectrometric characterization and physiological actions of VPNDWAHFRGSWamide, a novel B type allatostatin in the crab, *Cancer borealis*. J Neurochem. 2007; 101(4):1099–1107. [PubMed: 17394556]

Goaillard JM, Schulz DJ, Kilman VL, Marder E. Octopamine modulates the axons of modulatory projection neurons. J Neurosci. 2004; 24(32):7063–7073. [PubMed: 15306640]

Goldberg D, Nusbaum MP, Marder E. Substance P-like immunoreactivity in the stomatogastric nervous systems of the crab *Cancer borealis* and the lobsters *Panulirus interruptus* and *Homarus americanus*. Cell Tiss Res. 1988; 252:515–522.

Golowasch J, Marder E. Proctolin activates an inward current whose voltage dependence is modified by extracellular Ca^{2+} J Neurosci. 1992; 12:810–817. [PubMed: 1347561]

Harris-Warrick RM, Marder E. Modulation of neural networks for behavior. Annu Rev Neurosci. 1991; 14:39–57. [PubMed: 2031576]

Harris-Warrick, RM.; Marder, E.; Selverston, AI.; Moulins, M. Dynamic Biological Networks. The Stomatogastric Nervous System. Cambridge: MIT Press; 1992. p. 328

Hauser F, Cazzamali G, Williamson M, Blenau W, Grimmelikhuijzen CJ. A review of neurohormone GPCRs present in the fruitfly Drosophila melanogaster and the honey bee Apis mellifera. Prog Neurobiol. 2006; 80(1):1–19. [PubMed: 17070981]

Huybrechts J, Nusbaum MP, Bosch LV, Baggerman G, De Loof A, Schoofs L. Neuropeptidomic analysis of the brain and thoracic ganglion from the Jonah crab, Cancer borealis. Biochem Biophys Res Commun. 2003; 308(3):535–544. [PubMed: 12914784]

Jansons IS, Cusson M, McNeil JN, Tobe SS, Bendena WG. Molecular characterization of a cDNA from Pseudaletia unipuncta encoding the Manduca sexta allatostatin peptide (Mas-AST). Insect Biochem Mol Biol. 1996; 26(8-9):767–773. [PubMed: 9014326]

Johnson EC, Bohn LM, Barak LS, Birse RT, Nassel DR, Caron MG, Taghert PH. Identification of Drosophila neuropeptide receptors by G protein-coupled receptors-beta-arrestin2 interactions. J Biol Chem. 2003; 278(52):52172–52178. [PubMed: 14555656]

Jorge-Rivera, JC. PhD Thesis. Neuroscience Graduate Program; 1997. Modulation of stomatogastric musculature in the crab *Cancer borealis*; p. 114

Jorge-Rivera JC, Sen K, Birmingham JT, Abbott LF, Marder E. Temporal dynamics of convergent modulation at a crustacean neuromuscular junction. J Neurophysiol. 1998; 80:2559–2570. [PubMed: 9819263]

Kastin, AJ., editor. Handbook of biologically active peptides. Burlington, MA: Academic Press, Elsevier Inc.; 2006.

Katz PS, Eigg MH, Harris-Warrick RM. Serotonergic/cholinergic muscle receptor cells in the crab stomatogastric nervous system. I. Identification and characterization of the gastropyloric receptor cells. J Neurophysiol. 1989; 62:558–570. [PubMed: 2769347]

Katz PS, Harris-Warrick RM. Serotonergic/cholinergic muscle receptor cells in the crab stomatogastric nervous system. II. Rapid nicotinic and prolonged modulatory effects on neurons in the stomatogastric ganglion. J Neurophysiol. 1989; 62:571–581. [PubMed: 2769348]

Kilman VL, Fénelon V, Richards KS, Thirumalai V, Meyrand P, Marder E. Sequential developmental acquisition of cotransmitters in identified sensory neurons of the stomatogastric nervous system of the lobsters, *Homarus americanus* and *Homarus gammarus*. J Comp Neurol. 1999; 408:318–334. [PubMed: 10340509]

Kilman VL, Marder E. Ultrastructure of the stomatogastric ganglion neuropil of the crab, *Cancer borealis*. J Comp Neurol. 1996; 374:362–375. [PubMed: 8906505]

Kim YJ, Bartalska K, Audsley N, Yamanaka N, Yapici N, Lee JY, Kim YC, Markovic M, Isaac E, Tanaka Y, Dickson BJ. MIPs are ancestral ligands for the sex peptide receptor. Proc Natl Acad Sci U S A. 2010; 107(14):6520–6525. [PubMed: 20308537]

Kramer SJ, Toschi A, Miller CA, Kataoka H, Quistad GB, Li JP, Carney RL, Schooley DA. Identification of an allatostatin from the tobacco hornworm *Manduca sexta*. Proc Natl Acad Sci U S A. 1991; 88(21):9458–9462. [PubMed: 1946359]

Kreissl S, Weiss T, Djokaj S, Balezina O, Rathmayer W. Allatostatin modulates skeletal muscle performance in crustaceans through pre- and postsynaptic effects. Eur J Neurosci. 1999; 11(7): 2519–2530. [PubMed: 10383641]

Kutz KK, Schmidt JJ, Li L. *In situ* tissue analysis of neuropeptides by MALDI FTMS in-cell accumulation. Anal Chem. 2004; 76(19):5630–5640. [PubMed: 15456280]

Kwok R, Rui Zhang J, Tobe SS. Regulation of methyl farnesoate production by mandibular organs in the crayfish, Procambarus clarkii: a possible role for allatostatins. J Insect Physiol. 2005; 51(4): 367–378. [PubMed: 15890179]

Ma M, Bors EK, Dickinson ES, Kwiatkowski MA, Sousa GL, Henry RP, Smith CM, Towle DW, Christie AE, Li L. Characterization of the *Carcinus maenas* neuropeptidome by mass spectrometry and functional genomics. General and comparative endocrinology. 2009a; 161(3):320–334. [PubMed: 19523386]

Ma M, Chen R, Sousa GL, Bors EK, Kwiatkowski MA, Goiney CC, Goy MF, Christie AE, Li L. Mass spectral characterization of peptide transmitters/hormones in the nervous system and neuroendocrine organs of the American lobster *Homarus americanus*. General and comparative endocrinology. 2008; 156(2):395–409. [PubMed: 18304551]

Ma M, Gard AL, Xiang F, Wang J, Davoodian N, Lenz PH, Malecha SR, Christie AE, Li L. Combining in silico transcriptome mining and biological mass spectrometry for neuropeptide discovery in the Pacific white shrimp *Litopenaeus vannamei*. Peptides. 2010; 31(1):27–43. [PubMed: 19852991]

Ma M, Szabo TM, Jia C, Marder E, Li L. Mass spectrometric characterization and physiological actions of novel crustacean C-type allatostatins. Peptides. 2009b; 30(9):1660–1668. [PubMed: 19505516]

Ma M, Wang J, Chen R, Li L. Expanding the Crustacean neuropeptidome using a multifaceted mass spectrometric approach. Journal of proteome research. 2009c; 8(5):2426–2437. [PubMed: 19222238]

Marder E, Bucher D. Understanding circuit dynamics using the stomatogastric nervous system of lobsters and crabs. Annu Rev Physiol. 2007; 69:291–316. [PubMed: 17009928]

Marder E, Calabrese RL. Principles of rhythmic motor pattern generation. Physiol Rev. 1996; 76:687–717. [PubMed: 8757786]

Marder E, Calabrese RL, Nusbaum MP, Trimmer B. Distribution and partial characterization of FMRFamide-like peptides in the stomatogastric nervous systems of the rock crab, *Cancer borealis*, and the spiny lobster, *Panulirus interruptus*. J Comp Neurol. 1987; 259:150–163. [PubMed: 3584554]

Marder E, Hooper SL, Siwicki KK. Modulatory action and distribution of the neuropeptide proctolin in the crustacean stomatogastric nervous system. J Comp Neurol. 1986; 243:454–467. [PubMed: 2869069]

Marder E, Thirumalai V. Cellular, synaptic and network effects of neuromodulation. Neural Netw. 2002; 15(4-6):479–493. [PubMed: 12371506]

Marder, E.; Weimann, JM. Modulatory control of multiple task processing in the stomatogastric nervous system. In: Kien, J.; McCrohan, C.; Winlow, B., editors. Neurobiology of Motor Progamme Selection. New York: Pergamon Press; 1992. p. 3-19.

Mayoral JG, Nouzova M, Brockhoff A, Goodwin M, Hernandez-Martinez S, Richter D, Meyerhof W, Noriega FG. Allatostatin-C receptors in mosquitoes. Peptides. 2010; 31(3):442–450. [PubMed: 19409436]

Mortin LI, Marder E. Differential distribution of ß-pigment dispersing hormone (ß-PDH)-like immunoreactivity in the stomatogastric nervous system of five species of decapod crustaceans. Cell Tiss Res. 1991; 265:19–33.

Nassel DR, Winther AM. Drosophila neuropeptides in regulation of physiology and behavior. Prog Neurobiol. 2010; 92(1):42–104. [PubMed: 20447440]

Nusbaum MP. Regulating peptidergic modulation of rhythmically active neural circuits. Brain Behav Evol. 2002; 60(6):378–387. [PubMed: 12563170]

Nusbaum MP, Beenhakker MP. A small-systems approach to motor pattern generation. Nature. 2002; 417(6886):343–350. [PubMed: 12015615]

Nusbaum MP, Blitz DM, Swensen AM, Wood D, Marder E. The roles of co-transmission in neural network modulation. Trends Neurosci. 2001; 24(3):146–154. [PubMed: 11182454]

Nusbaum MP, Marder E. A modulatory proctolin-containing neuron (MPN). I. Identification and characterization. J Neurosci. 1989a; 9:1591–1599. [PubMed: 2566658]

Nusbaum MP, Marder E. A modulatory proctolin-containing neuron (MPN). II. State-dependent modulation of rhythmic motor activity. J Neurosci. 1989b; 9:1600–1607. [PubMed: 2566659]

Pratt GE, Farnsworth DE, Siegel NR, Fok KF, Feyereisen R. Identification of an allatostatin from adult *Diploptera punctata*. Biochem Biophys Res Commun. 1989; 163:1243–1247. [PubMed: 2783135]

Skiebe P. Allatostatin-like immunoreactivity within the stomatogastric nervous system and the pericardial organs of the crab *Cancer pagurus*, the lobster *Homarus americanus*, and the crayfish *Cherax destructor* and *Procambarus clarkii*. J Comp Neurol. 1999; 403:85–105. [PubMed: 10075445]

Skiebe P, Ganeshina O. Synaptic neuropil in nerves of the crustacean stomatogastric nervous system: an immunocytochemical and electron microscopical study. J Comp Neurol. 2000; 420(3):373–397. [PubMed: 10754509]

Skiebe P, Schneider H. Allatostatin peptides in the crab stomatogastric nervous system: inhibition of the pyloric motor pattern and distribution of allatostatin-like immunoreactivity. J Exp Biol. 1994; 194:195–208. [PubMed: 7964402]

Skiebe P, Wollenschlager T. Putative neurohemal release zones in the stomatogastric nervous system of decapod crustaceans. J Comp Neurol. 2002; 453(3):280–291. [PubMed: 12378588]

Stay B, Chan KK, Woodhead AP. Allatostatin-immunoreactive neurons projecting to the corpora allata of adult *Diploptera punctata*. Cell Tissue Res. 1992; 270:15–23. [PubMed: 1423517]

Stay B, Tobe SS. The role of allatostatins in juvenile hormone synthesis in insects and crustaceans. Annu Rev Entomol. 2007; 52:277–299. [PubMed: 16968202]

Stein W. Modulation of stomatogastric rhythms. J Comp Physiol A Neuroethol Sens Neural Behav Physiol. 2009; 195(11):989–1009. [PubMed: 19823843]

Stemmler EA, Bruns EA, Cashman CR, Dickinson PS, Christie AE. Molecular and mass spectral identification of the broadly conserved decapod crustacean neuropeptide pQIRYHQCYFNPISCF: the first PISCF-allatostatin (Manduca sexta- or C-type allatostatin) from a non-insect. General and comparative endocrinology. 2009; 165(1):1–10. [PubMed: 19467234]

Stemmler EA, Bruns EA, Cashman CR, Dickinson PS, Christie AE. Molecular and mass spectral identification of the broadly conserved decapod crustacean neuropeptide pQIRYHQCYFNPISCF: the first PISCF-allatostatin (Manduca sexta- or C-type allatostatin) from a non-insect. General and comparative endocrinology. 2010; 165(1):1–10. [PubMed: 19467234]

Swensen AM, Golowasch J, Christie AE, Coleman MJ, Nusbaum MP, Marder E. GABA and responses to GABA in the stomatogastric ganglion of the crab *Cancer borealis*. J Exp Biol. 2000; 203(Pt):2075–2092. [PubMed: 10862721]

Swensen AM, Marder E. Multiple peptides converge to activate the same voltage-dependent current in a central pattern-generating circuit. J Neurosci. 2000; 20(18):6752–6759. [PubMed: 10995818]

Swensen AM, Marder E. Modulators with convergent cellular actions elicit distinct circuit outputs. J Neurosci. 2001; 21:4050–4058. [PubMed: 11356892]

Thirumalai V, Marder E. Colocalized neuropeptides activate a central pattern generator by acting on different circuit targets. J Neurosci. 2002; 22:1874–1882. [PubMed: 11880517]

Tobe SS, Bendena WG. The regulation of juvenile hormone production in arthropods. Functional and evolutionary perspectives. Ann N Y Acad Sci. 1999; 897:300–310. [PubMed: 10676458]

Vedel JP, Moulins M. A motor neuron involved in two centrally generated motor patterns by means of two different spike initiating sites. Brain Res. 1977; 138(2):347–352. [PubMed: 201348]

Veenstra JA. Allatostatin C and its paralog allatostatin double C: the arthropod somatostatins. Insect Biochem Mol Biol. 2009; 39(3):161–170. [PubMed: 19063967]

Weaver RJ, Audsley N. Neuropeptide regulators of juvenile hormone synthesis: structures, functions, distribution, and unanswered questions. Ann N Y Acad Sci. 2009; 1163:316–329. [PubMed: 19456353]

Williamson M, Lenz C, Winther AM, Nassel DR, Grimmelikhuijzen CJ. Molecular cloning, genomic organization, and expression of a B-type (cricket-type) allatostatin preprohormone from *Drosophila melanogaster*. Biochem Biophys Res Commun. 2001; 281(2):544–550. [PubMed: 11181081]

Woodhead AP, Stay B, Seidel SL, Khan MA, Tobe SS. Primary structure of four allatostatins: neuropeptide inhibitors of juvenile hormone synthesis. Proc Natl Acad Sci USA. 1989; 86:5997–6001. [PubMed: 2762309]

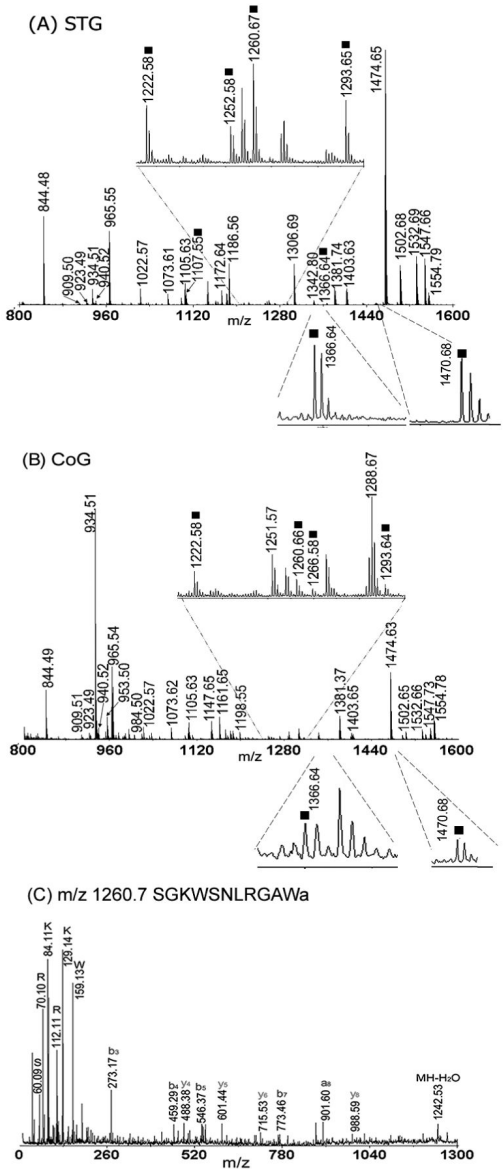

Figure 1.

Direct tissue analysis of ganglia in the STNS. Mass spectra were obtained from a small piece of tissue from the STG (**A**) and CoG (**B**). Many peptides were detected, including B-type CbASTs (indicated with squares). **C.** Example of an MS/MS spectra for CbAST-B3 SGKWSNLRGAWa (m/z 1260.7) from direct tissue analysis of one STG; a, b and y ions are indicated.

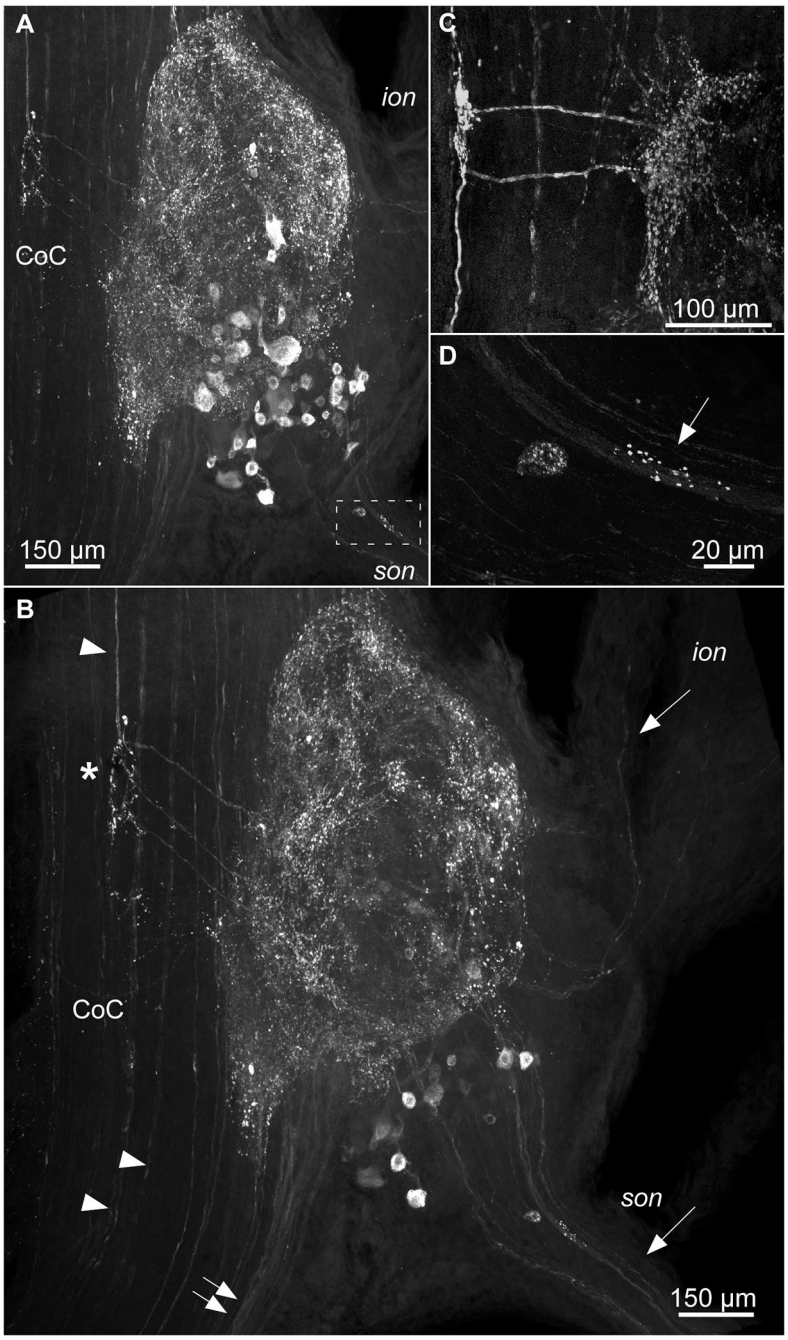

Figure 2.

CbAST-B1-like staining in the CoG. **A**. Maximum intensity projection. Immunoreactivity was seen in CoG cell bodies as well as in the neuropil. Immunoreactive fibers were apparent in the *son* and *ion*. Cell bodies and punctate labeling were often detected at the beginning of the *son* (boxed region). **B**. Mid-ganglion view of CbAST-B1-LI in the same ganglion as (**A**) emphasizing the presence of processes leading from the CoC into the CoG (asterisk). Fibers in the CoC also bypassed the CoG (arrowheads). Immunoreactive fibers in the *son* and *ion* (arrows) extended into the CoG neuropil. Fibers were also visible traveling between the brain and CoG neuropil in the CoC (double arrows). **C**. Another preparation, high magnification of fibers extending perpendicularly from the CoC fiber pathway to the CoG

neuropil. Note in this case, two fibers can be seen extending to and branching out in the CoG neuropil. **D**. A cell and punctate staining in *son* (see boxed region in **A**).

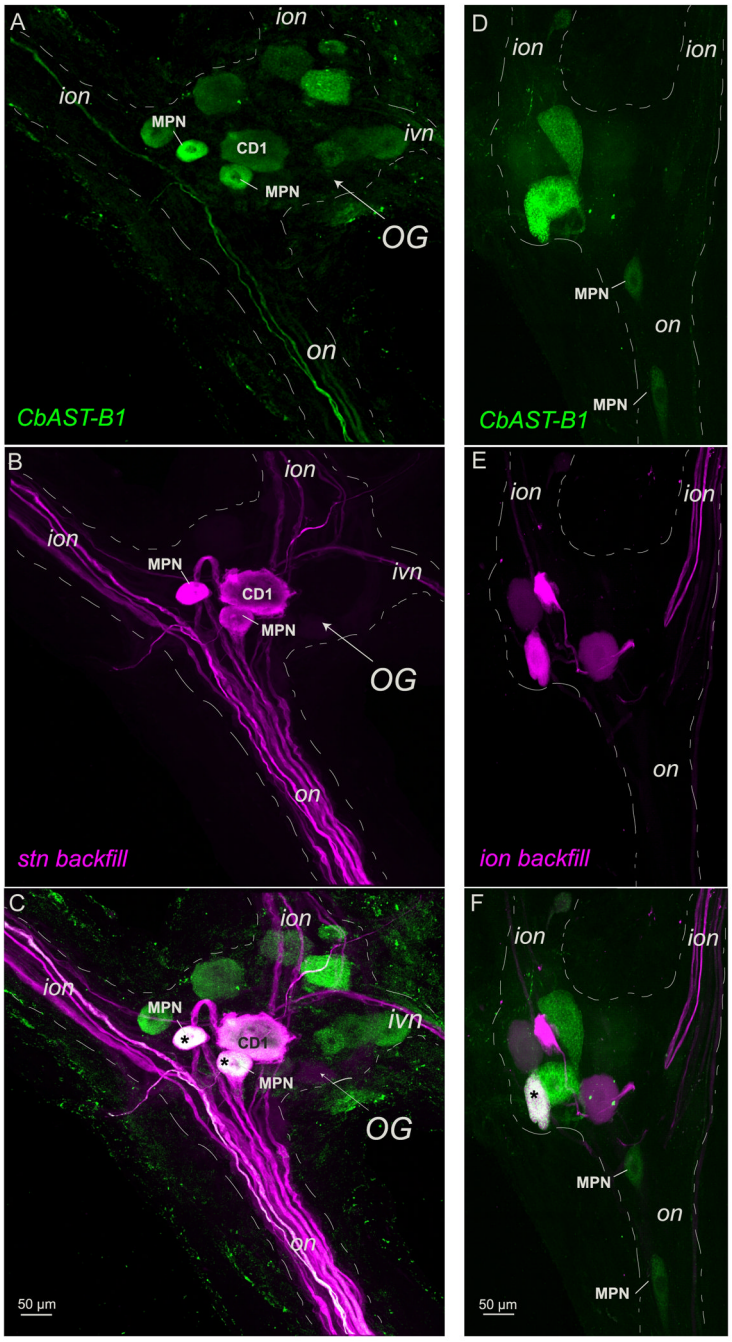

Figure 3.

CbAST-B1-like AST antibody staining in the OG and nerve backfills **A-C.** Neurobiotin backfill of the *stn* shows strong CbAST-B1-LI in both MPN somata (asterisks) and weak CbAST-B1-LI in the CD1 soma. Maximal intensity projections. **D-F.** Rhodamine-dextran backfill of the right *ion* labels 5 cells in the OG, of which one (asterisk) is strongly CbAST-B1-like immunoreactive. Maximal intensity projections.

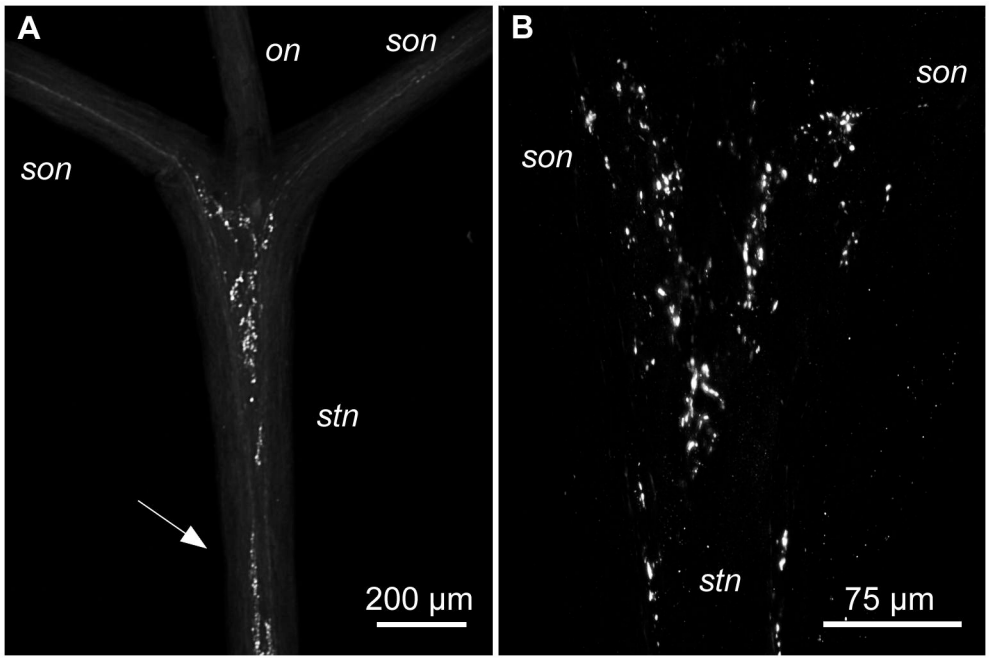

Figure 4.

CbAST-B1-LI in the anterior *stn*. **A.** Overview of the anterior *stn* and its junction with the two *sons* and the *on*. A large region of punctate staining is present in the anterior region of the *stn*. Fibers project from the two *sons* into the *stn*. Similar punctate staining was also detected in more posterior regions (arrow). **B.** High magnification of the anterior region of the *stn* from another preparation showing extensive punctate staining.

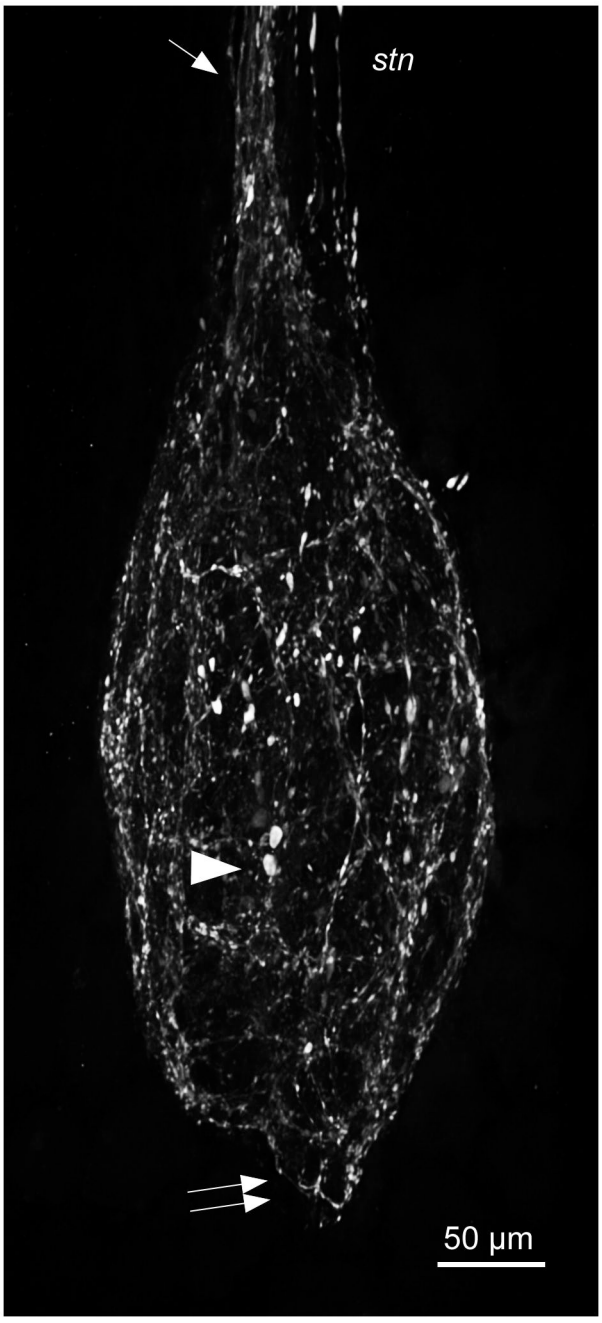

Figure 5.
CbAST-B1 staining in the STG is restricted to the neuropil. STG somata were not immunoreactive while fibers in the neuropil stained extensively. Bulbous structures measuring up to ~10 μm in length were detected in the central neuropil (arrowhead). Staining in the *stn* as it enters the STG is localized to one side of the nerve (single arrow). Fibers extended posteriorly into the *dvn* (double arrows).

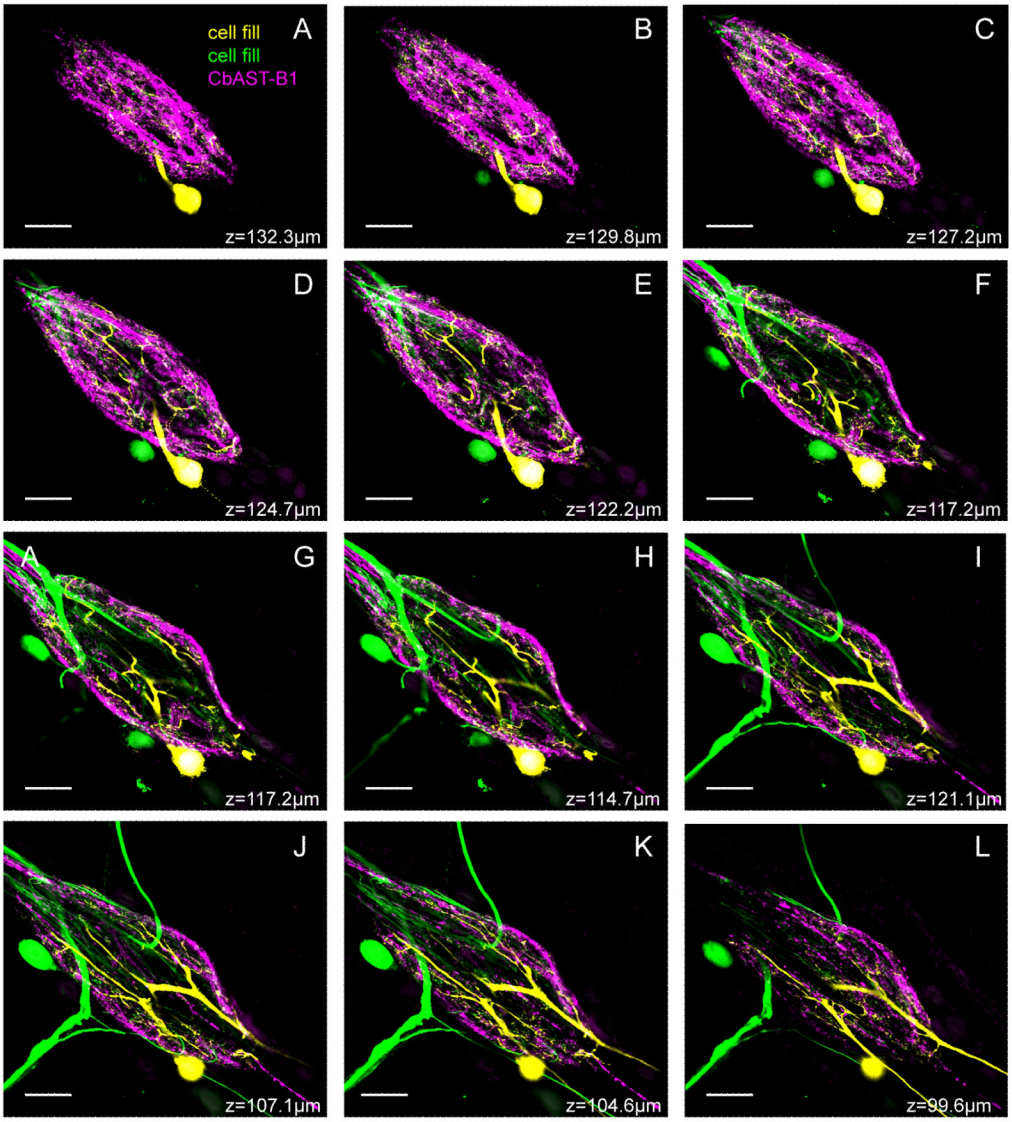

Figure 6.
Series of 2.5 μm-thick optical slices in a Z-stack of CbAST-B1-LI in the STG, with two dye-filled neurons. CbAST-B1-LI (magenta) was strongest around the periphery of the neuropil and virtually absent near the large diameter processes of the coarse, central neuropil. A VD cell was filled with Alexa Fluor 568 hydrazide (yellow), and a second, unidentified cell was filled with neurobiotin (green).

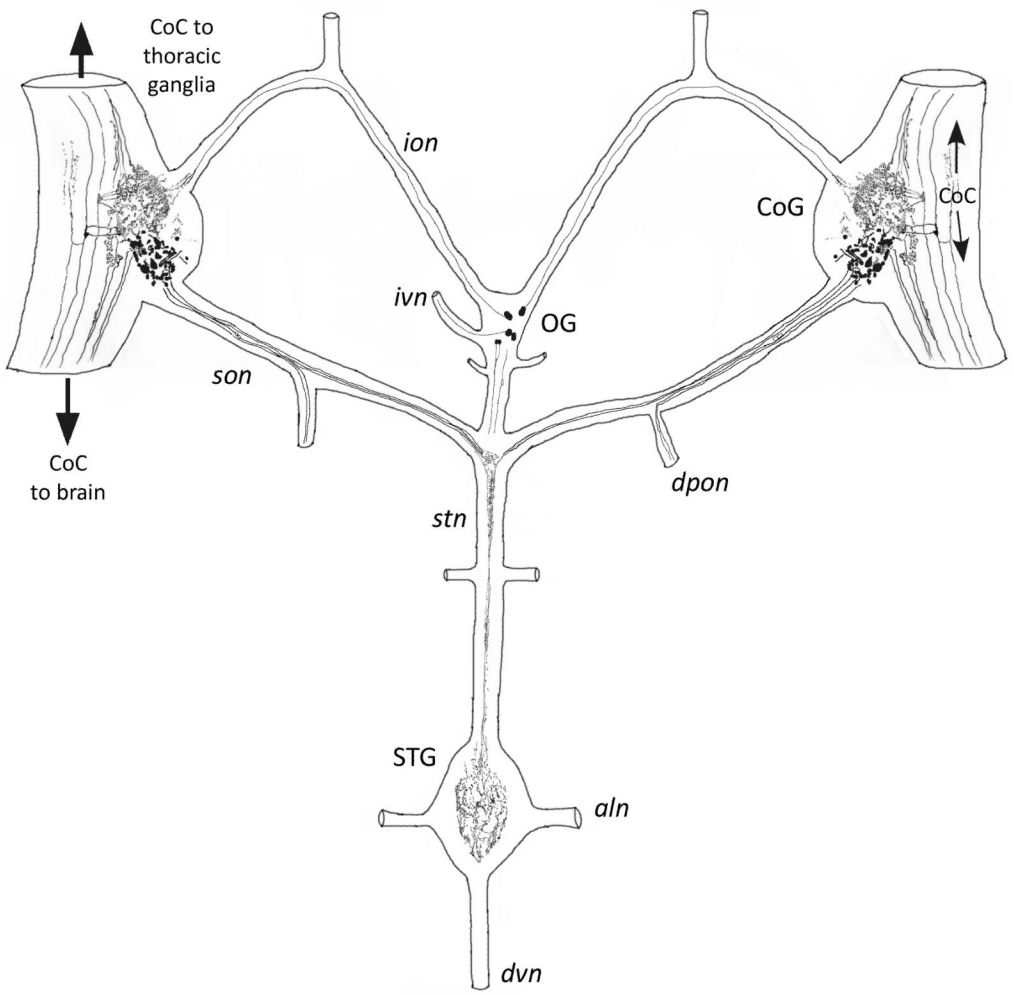

Figure 7.
Summary of CbAST-B1-LI in the STNS of *C. borealis*.

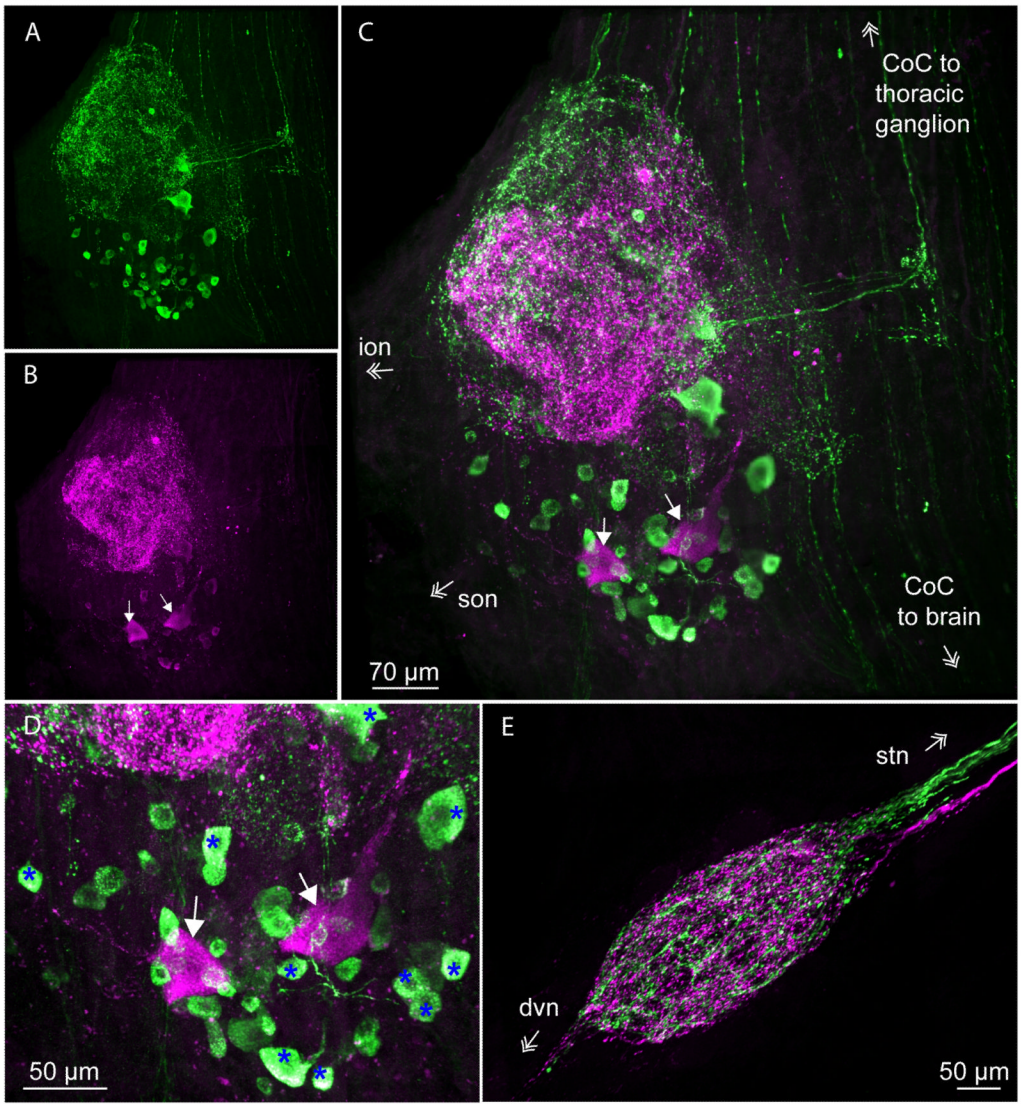

Figure 8.

CbAST-B1 and Dippu-AST 7 (A-type AST) immunoreactivity in the STNS. A. Maximal intensity projection of CbAST-B1-like staining in the CoG. Staining was detected in both cell bodies and neuropil. B. Maximal intensity projection of A-type AST staining in the same preparation. Arrows point to two large somata that were labeled. C. Overlay of A and B. D. Cell bodies in the CoG from the preparation in (C), showing some neurons colocalize the two families of peptides. Overlay of green and magenta in these somata appears white (blue asterisks). E. Maximal intensity projection of both CbAST-B1 (green) and Dippu-AST 7 (magenta) staining in the STG showing segregation of fiber staining in the *stn* and neuropil.

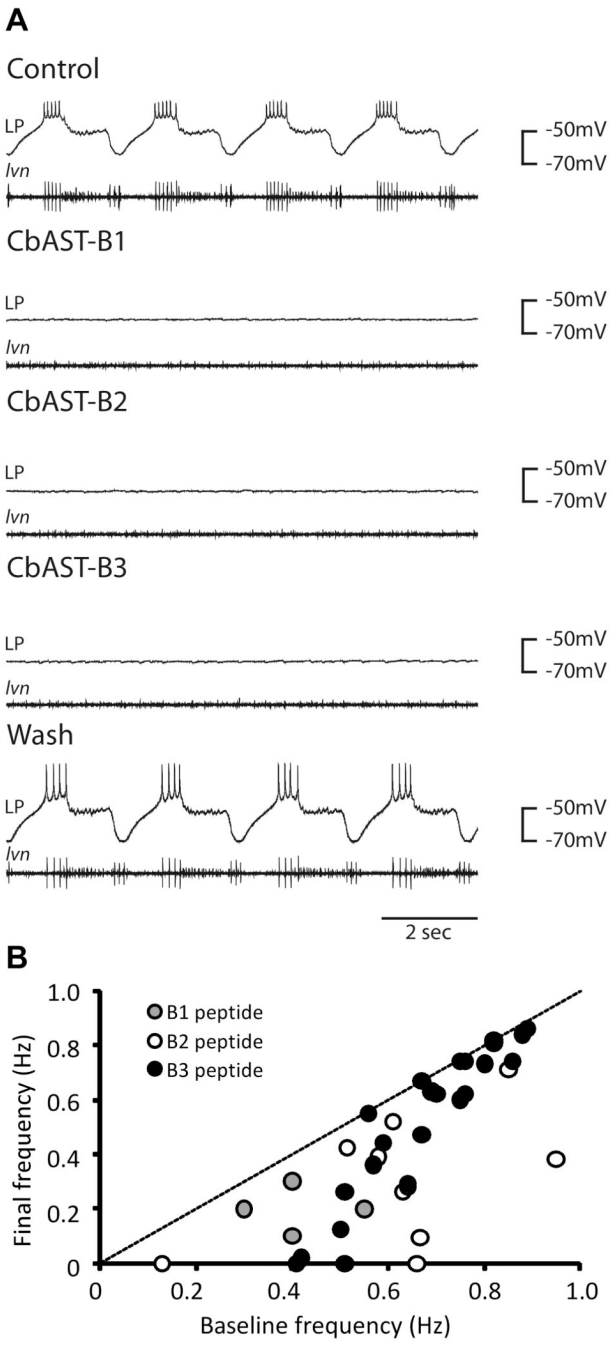

Figure 9.

Physiological effects of CbAST-B1, CbAST-B2, and CbAST-B3 on the pyloric rhythm. **A**. Effects of 10^{-5} M peptides on the pyloric rhythm. Representative intracellular recordings from the lateral pyloric (LP) neuron (top trace) and the corresponding extracellular recording from the lateral ventricular nerve (*lvn*, bottom trace), showing the activity of the PD (medium units), LP (largest unit), and PY (smallest unit) neurons. Application of either 10^{-5} M CbAST-B1, 10^{-5} M CbAST-B2 or 10^{-5} M CbAST-B3 resulted in hyperpolarization of the LP neuron and silencing of the pyloric rhythm. **B**. Plot of initial pyloric burst frequency vs. final burst frequency for preparations exposed to either 10^{-8} M CbAST-B1, 10^{-8} M CbAST-B2, 10^{-8} M CbAST-B3 plotted to show the burst frequency in the presence

of the peptide as a function of the preparation's initial frequency (n=37). Preparations with a more rapid initial frequency responded less to peptide application that those with a slower initial burst frequency (Mann-Whitney Rank Sum Test, p=0.002).

Table 1

Primary Antibodies used

Antigen	Immunogen	Manufacturer	Dilution
CbAST-B1	Synthetic peptide: BSA-linked B-AST, VPNDWAHFRGSW	Lampire Biological Laboratories, rabbit polyclonal, #7905	1:500-1:1,000
Dippu-AST-7	Synthetic peptide: BSA-linked Diploptera punctata allatostatin 7 (formerly I), APSGAQRLYGFGL-NH2	Developmental Studies Hybridoma Bank (U Iowa), mouse monoclonal, #5F10	1:1000
CabTRP	C-terminal BSA-linked substance P	Accurate Chemical and Scientific (Westbury, NY), rat monoclonal [NC1/34 HL]	1:300

Table 2

List of allatostatins present in the STNS

Peptide Name	$[M+H]^+$	Peptide sequences	STG	CoG	*stn*
CbAST-B1	1470.7	VPNDWAHFRGSWa	6	4	2
CbAST-B2	1107.5	QWSSMRGAWa	6	4	2
CbAST-B3	1260.6	SGKWSNLRGAWa	6	5	2
CbAST-B4	1165.6	NWNKFQGSWa	5	2	2
CbAST-B5	1182.6	TSWGKFQGSWa	1	NA	
CbAST-B6	1222.6	GNWNKFQGSWa	5	5	2
CbAST-B7	1252.6	NNWSKFQGSWa	5	1	2
CbAST-B8	1293.6	STNWSSLRSAWa	6	3	2
CbAST-B9	1366.6	NNNWSKFQGSWa	5	2	2

Note: Numbers represent how many preparations each peptide was detected in, out of a total of 6.

J Comp Neurol. Author manuscript; available in PMC 2012 September 1.